IEEE Access
Multidisciplinary : Rapid Review : Open Access Journal

Received 31 March 2023, accepted 15 May 2023, date of publication 25 May 2023, date of current version 8 June 2023.

Digital Object Identifier 10.1109/ACCESS.2023.3280070

RESEARCH ARTICLE

Aggregation of Multi-Agent System on Manifolds With Riemannian Geometry

LUNXIAO TANG, TAO YU, AND MAOKANG LUO
College of Mathematics, Sichuan University, Chengdu 610065, China
Corresponding author: Tao Yu (scuyutao@163.com)

ABSTRACT In this work, we establish a novel dynamical model to address the aggregation problem of the multi-agent system on manifolds. At first, with the help of local coordinate charts, we describe the multi-agent system as a manifold, which is part of the ambient space. Then, we convert the aggregation problem of agents into an optimization issue to minimize the volume of a virtual manifold, and we show that evolving along its mean curvature field can minimize the virtual manifold's volume. Finally, we implement our approach for the multi-agent system on the sphere and non-homogeneous manifold. Several numerical simulations are also performed to verify our theoretical analysis.

INDEX TERMS Aggregation, minimal volume, multi-agent system, Riemannian geometry, synergistic behaviors.

I. INTRODUCTION

Synergistic behaviors of multi-agent systems are ubiquitous in our natural and manufactured complex systems and have many features such as aggregation, velocity alignment, and collision avoidance. In the case of Euclidean space, the emergence of synergistic behaviors has been extensively studied in plenty of works such as the pivotal Artificial Potential Field model in [1] and [2], the Vicsek type model in [3], [4], and [5], the Kuramoto type model in [6], [7], and [8] and the Cucker-Smale (C-S) type model in [9]. Nevertheless, such models barely consider the curvature effects of the space, which may affect the emergence of synergistic behaviors of multi-agent systems moving in a more complicated manifold. In more recent years, the emergence of synergistic behaviors of multi-agent systems on manifolds has been an active field of interest due to its numerous applications in manufacturing, aerospace technologies, and robotics. In order to address this problem, models dealing with aggregation, velocity alignment, and collision avoidance on manifolds have been proposed. In order to realize the aggregation of multi-agent systems on sphere, a second-order dynamic model based on the classic Kuramoto model is introduced in [6], [10], and [8]. In order to achieve velocity alignment of multi-agent systems on various manifolds, an extended Cucker-Smale (C–S) model is provided in [11], [12], and [13]. The collisions avoidance task of a multi-agent system on general manifolds has been considered in [14], [15], [16], [17], and [18], and an artificial potential on a general manifold is designed to ensure that agents will avoid collisions within some desired tolerance. In general, these models cannot describe all of the significant features of synergistic behaviors of multi-agent systems entirely, and some of their applications are limited.

However, the second-order dynamic model in [10] has many deficiencies. Firstly, the multi-agent system and ambient space need to be embedded in a Euclidean space, and the evolution of agents is described by the global descartes coordinate chart. Therefore, the dynamical system of agents has to satisfy some specific form due to geometric constraints. Besides, it is difficult to keep the agents moving in the ambient space when the dynamical system is solved numerically. Last but not least, the Kuramoto-type models can not be implemented on other manifolds except sphere and some specific cases. In order to address these deficiencies, a general framework based on Riemannian geometry is introduced by us to realize multi-agent systems' aggregation on manifolds. In order to make the agents continuously evolve in the ambient space, we use local charts to describe the multi-agent system, and the agents are naturally part of the ambient

The associate editor coordinating the review of this manuscript and approving it for publication was Jason Gu.

space. Furthermore, we convert the aggregation problem of the agents into an optimization problem of minimizing the volume of a specific manifold. Then, we find out the desired direction to minimize the virtual manifold's volume and establish a novel dynamic model to describe the aggregation behavior of agents on manifolds.

In summary, we convert a multi-objective optimization problem (swarm's aggregation and shortest path length) under geometric constraints into a problem of minimizing the volume of a manifold, and we realize swarm's cooperative aggregation behaviors on the unit sphere and a curved surface similar to a hilly terrain; compared to previous research, our method and theory are more proper and practicable for engineering implementations. The remainder of this paper is structured as follows. In section II, preliminaries on Riemannian geometry are introduced, and some concepts describing the movement in Euclidean space are interpreted in the language of Riemannian geometry. Section III deals with the proof of our main theoretical results and the construction of our model. Then, in section IV, we implement our approach for the multi-agent systems on the sphere and on a non-homogeneous manifold. Several numerical simulations are also performed by us to verify our approach's rationality. Finally, section V is devoted to a summary of our main results and discussing some remaining open problems for future work.

II. REVIEW OF RIEMANNIAN GEOMETRY

In this section, some standard concepts and symbols from Riemannian geometry that are used in the sequel are presented. Moreover, concepts in mechanics are reinterpreted in the language of Riemannian geometry, such as velocity, acceleration, and evolution of agents.

In our approach, the multi-agent system is treated as a manifold, denoted as $\mathcal{M}$. Each manifold is locally homeomorphic to a Euclidean space with the same dimension. Therefore, for any given point p belongs to $\mathcal{M}$ we can find a homeomorphism ζ on a local neighborhood U, and ζ determine the one-to-one correspondence between U and the Euclidean space. According to the correspondence, each point in U is designated a unique Euclidean coordinate denoted as $\{x^i\}_{i=1}^n$, n is the dimension of $\mathcal{M}$. If ζ is infinitely differentiable, which means $\zeta \in C^\infty(\mathcal{M})$, then $\mathcal{M}$ is called a smooth manifold. $\{x^i\}_{i=1}^n$ is called the local chart on U, and the tangent space of $\mathcal{M}$ is defined to be $T_p\mathcal{M} = \{\frac{\partial}{\partial x^1}, \frac{\partial}{\partial x^2}, \cdots, \frac{\partial}{\partial x^n}\}$. The union $T\mathcal{M} = \bigcup_{p\in\mathcal{M}} T_p\mathcal{M}$ is called the tangent bundle of $\mathcal{M}$. A vector field defined on $\mathcal{M}$ is denoted as $X = \sum_{i=1}^{n} X_i \frac{\partial}{\partial x^i}$ and $X_p \in T_p\mathcal{M}, \forall p \in \mathcal{M}$, the union of the vector fields is $\mathfrak{T}\mathcal{M}$.

1) **Riemann metric tensor**
For any manifold $\mathcal{M}$ the inner product of tangent bundle vectors is determined by a second order non-negative symmetric tensor g_{ij} called the metric tensor of $\mathcal{M}$, and each component is defined by $g_{ij} = \langle \frac{\partial}{\partial x^i}, \frac{\partial}{\partial x^j} \rangle$.

2) **Velocity and acceleration of agents on manifolds**
The velocity v of an agent on any point p of manifold $\mathcal{M}$ is a tangent vector, which lies in $T\mathcal{M}$, and the acceleration of the agent is defined by the covariant derivatives on $\mathcal{M}$. The covariant derivative of any two vector field is defined as follow:

$$\mathrm{D}_X Y = \sum_{i,j,k=1}^{n} (X_i \frac{\partial Y_k}{\partial x^i} + \Gamma_{ij}^k X_i Y_j) \frac{\partial}{\partial x^k} \tag{1}$$

where the Riemann connection coefficients Γ_{ij}^k are calculated from the Riemannian metric and its derivatives:

$$\Gamma_{ij}^k = \frac{1}{2} g^{kl} (\partial_i g_{jl} + \partial_j g_{il} - \partial_l g_{ij}). \tag{2}$$

Moreover, the covariant derivative along a curve $\gamma(t) \subset \mathcal{M}$ is defined as follow:

$$\begin{aligned} \mathrm{D}_t V &= \dot{V}^j \frac{\partial}{\partial x^j} + V^j \mathrm{D}_{\dot{\gamma}} \frac{\partial}{\partial x^j} \\ &= (\dot{V}^k + V^j \dot{\gamma}^i \Gamma_{ij}^k) \frac{\partial}{\partial x^k}. \end{aligned} \tag{3}$$

If we substitute the tangent vector of γ as the velocity v of the agent, then we will get the acceleration of the agent $D_v v = (\dot{v}^k + v^j \dot{v}^i \Gamma_{ij}^k) \frac{\partial}{\partial x^k}$ on manifold.

3) **Evolution of the multi-agent systems described by the smooth flow map**
In order to describe the evolution of the multi-agent systems in nonlinear space, a smooth flow map from $\mathcal{M} \times [0, T]$ to the ambient space is naturally defined to be (the same definition in [19])

$$\Phi : \mathcal{M} \times [0, T] \to \mathcal{E}$$
$$\Phi_t(\mathcal{M}) = \mathcal{M}_t \subset \mathcal{E}.$$

and the velocity of agents is exactly the pushforward (the same definition in [21]) of the tangent vector $\frac{\partial}{\partial t}$, which is $W_t = (\Phi_t)_*(\frac{\partial}{\partial t})$. The volume of the system at time t is exactly the volume of submanifold $\mathcal{M}_t$, that is $V(t) = \int_{\mathcal{M}_t} \mathrm{d}\Omega_t$, where Ω_t is the volume element of $\mathcal{M}_t$.

4) **Length of the track of an agent on manifolds**
The track of an agent is described by a smooth curve γ on the manifold, which is defined by an infinitely differentiable map on the manifold $\gamma : t \in [0, 1] \to \mathcal{M}$. The length of the track is

$$L(\gamma(t)) = \int_0^1 \sqrt{g_{ij}(t)\dot{\gamma}^i(t)\dot{\gamma}^j(t)} \mathrm{d}t. \tag{4}$$

where g_{ij} is the Riemannian metric tensor of the manifold, and $\dot{\gamma}^i(t)$, $\dot{\gamma}^j(t)$ are the i-th and j-th component of the tangent vector of the curve at time t.

5) **Gauss formula formula of submanifold**
There is a significant formula for submanifold in Riemannian geometry, which will be used in the sequel proof. The Gauss formula for submanifold is as follow:

$$\overline{\mathrm{D}}_{F_* Y} F_*(X) = F_*(\mathrm{D}_Y X) + h(X, Y), \ \forall X, Y \in \mathfrak{T}(\mathcal{M}). \tag{5}$$

TABLE 1. Nomenclature.

Symbol	Description
Φ	Smooth flow map of swarm
$\mathcal{M}$	Manifold of swarm
$\widetilde{\mathcal{M}}$	Virtual manifold
N	Number of agents
n	Dimension of $\mathcal{M}$ and $\widetilde{\mathcal{M}}_t$
T	Final time
D_X^Y	Covariant derivative
g_{ij}	Riemannian metric
Γ_{ij}^k	Christoffel symbol
$\mathcal{H}_t$	Mean curvature vector field
V	Volume of $\mathcal{M}$
$\widetilde{V}$	Volume of $\widetilde{\mathcal{M}}$

All of this preliminaries listed can be found in the references [20], [21], [22], and the nomenclature used in this paper is given in Table 1.

III. AGGREGATION OF THE MULTI-AGENT SYSTEM WITH THE MEAN CURVATURE FIELD

In the Artificial Potential Field model [2], a virtual artificial potential field $U_{art}(x)$ is constructed to control the motion of the agent. The agents move in the direction of the gradient of $U_{art}(x)$, which is called virtual forces $F_{art}(x)$. Inspired by the philosophy of the Artificial Potential Field approach, we construct time-varying virtual manifolds $\widetilde{\mathcal{M}}_t$ for the multi-agent systems and use virtual manifold's volume $\widetilde{V}(t)$ to describe the state of the system. $\widetilde{V}(t)$ play the role as that the artificial potential $U_{art}(x)$ plays in Artificial Potential Field approach. Similar to the motion of agents in a potential field tends to minimize the potential functions $U_{art}(x)$, the evolution of agents in our approach tends to minimize the volume of the virtual manifolds $\widetilde{\mathcal{M}}_t$.

There are two main procedures in our approach. At first, we figure out that the direction of the mean curvature vector will minimize $\widetilde{V}_t$ after some calculations. Then, the mean curvature vector is projected into the tangent space of $\mathcal{M}_t$, and the model is finally attained by taking the length of the track into consideration. The first subsection is devoted to proving that evolution in the direction of the mean curvature vector will minimize the volume of $\widetilde{\mathcal{M}}_t$.

A. MINIMIZATION OF THE VOLUME OF THE VIRTUAL MANIFOLD $\widetilde{\mathcal{M}}_t$

Our approach treats the multi-agent system as a manifold $\mathcal{M}$ in ambient space. Firstly, we construct some specific virtual manifolds $\widetilde{\mathcal{M}}_t$ concerned with different problems, such as obstacle avoidance, velocity alignment, and enclosing a target. Then, in order to obtain the smooth flow map Ψ for agents, we need to attain $\widetilde{\Psi}$ at first. The key is to find the velocity field of $\widetilde{\Psi}$, which minimizes the volume $\widetilde{V}_t$ of the virtual manifold $\widetilde{\mathcal{M}}_t$. Following this train of thought, we try to find the direction that will minimize the volume of a virtual manifold in the sequel.

Evolution of the virtual manifold $\widetilde{\mathcal{M}}_t$ is described by a smooth flow map defined as follows:

$$\begin{aligned}\widetilde{\Phi} &: \widetilde{\mathcal{M}} \times [0, T] \to \mathcal{E},\\ \widetilde{\Phi}_t(\widetilde{\mathcal{M}}) &= \widetilde{\mathcal{M}}_t \subset \mathcal{E}.\end{aligned} \tag{6}$$

The velocity field of the virtual manifold is exactly the pushforward (defined in [19]) of the tangent vector $\frac{\partial}{\partial t}$, which is $\widetilde{W}_t = (\widetilde{\Phi}_t)_*(\frac{\partial}{\partial t})$. The volume of the virtual manifold at time t is $\widetilde{V}(t) = \int_{\widetilde{\mathcal{M}}_t} \mathrm{d}\widetilde{\Omega}_t$, where $\widetilde{\Omega}_t$ is the volume element of $\widetilde{\mathcal{M}}_t$. Then, the desired velocity vector field for the virtual manifold $\widetilde{\mathcal{M}}_t$ is $\widetilde{W}_t \in \mathfrak{T}\mathcal{M}_t$.

We prove that if $\widetilde{W}_t = \mathcal{H}_t$, then the volume $\widetilde{V}(t)$ of the virtual manifold will decay and converge to a non-negative constant. The process to attain the results is shown in the proof of Theorem 1:

Theorem 1: If the velocity field $(\widetilde{\Phi}_t)_*(\frac{\partial}{\partial t}) = \widetilde{W}_t$ of the virtual manifold is $\alpha\mathcal{H}_t$, $\langle \mathcal{H}_t, \mathcal{H}_t\rangle > 0, \alpha > 0$ and $\partial\widetilde{\mathcal{M}}_t = \varnothing$, for arbitrary $t \in [0, +\infty)$, then the volume $\widetilde{V}(t)$ of the virtual manifold $\widetilde{\mathcal{M}}_t$ will decay monotonically.

Proof: The first-order derivative of volume of the virtual manifold $\widetilde{V}'(t)$ is computed as follow:

$$\begin{aligned}\widetilde{V}'(t) &= \frac{\partial \int_{\widetilde{\mathcal{M}}_t} \mathrm{d}\widetilde{\Omega}_t}{\partial t}\\ &= \int_{\widetilde{\mathcal{M}}_t} \frac{\partial\sqrt{\widetilde{G}_t}}{\partial t}\mathrm{d}u^1 \wedge \cdots \wedge \mathrm{d}u^n\\ &= \int_{\widetilde{\mathcal{M}}_t} \frac{1}{2\sqrt{\widetilde{G}_t}}\frac{\partial\widetilde{G}_t}{\partial t}\mathrm{d}u^1 \wedge \cdots \wedge \mathrm{d}u^n\\ &= \int_{\widetilde{\mathcal{M}}_t} \frac{1}{2\sqrt{\widetilde{G}_t}}(\sum_{i,j}(\widetilde{a}_t)_{ij}\frac{\partial(\widetilde{g}_t)_{ij}}{\partial t})\mathrm{d}u^1 \wedge \cdots \wedge \mathrm{d}u^n\\ &= \frac{1}{2}\int_{\widetilde{\mathcal{M}}_t} \sum_{i,j}(\widetilde{g}_t)^{ij}\frac{\partial(\widetilde{g}_t)_{ij}}{\partial t}\mathrm{d}\widetilde{\Omega}_t.\end{aligned} \tag{7}$$

where $\{u^i\}_{i=1}^n$ is the local coordination of virtual manifold, $\widetilde{\Omega}_t = \sqrt{\widetilde{G}_t}\mathrm{d}u^1 \wedge \cdots \wedge \mathrm{d}u^n$, $\widetilde{G}_t$ is the determinant of the corresponding metric matrix $(\widetilde{g}_t)^{ij}$. $(\widetilde{a}_t)_{ij}$ is the cofactor of $(\widetilde{g}_t)_{ij}$ in the determinant $\widetilde{G}_t$, $(\widetilde{g}_t)^{ij}$ is the i,j-th element of the inverse of the metric matrix $\widetilde{g}_t$.
Since

$$\begin{aligned}\frac{\partial(\widetilde{g}_t)_{ij}}{\partial t} &= \frac{\partial\langle(X_t)_i, (X_t)_j\rangle}{\partial t}\\ &= \langle\overline{\mathrm{D}}_{\frac{\partial}{\partial t}}(X_t)_i, (X_t)_j\rangle + \langle(X_t)_i, \overline{\mathrm{D}}_{\frac{\partial}{\partial t}}(X_t)_j\rangle,\end{aligned} \tag{8}$$

where $(X_t)_i = (\widetilde{\Phi}_t)_*(\frac{\partial}{\partial u^i})$,and $\overline{\mathrm{D}}$ is the covariant derivative in the ambient space, we have

$$\widetilde{V}'(t) = \int_{\widetilde{\mathcal{M}}_t} \sum_{i,j}(\widetilde{g}_t)^{ij}\langle\overline{\mathrm{D}}_{\frac{\partial}{\partial t}}(X_t)_i, (X_t)_j\rangle\mathrm{d}\widetilde{\Omega}_t. \tag{9}$$

Using the equation

$$\begin{aligned}\overline{\mathrm{D}}_{\frac{\partial}{\partial t}}(X_t)_i &= \overline{\mathrm{D}}_{\frac{\partial}{\partial u^i}}\widetilde{W}_t + (\widetilde{\Phi}_t)_*([\frac{\partial}{\partial t}, \frac{\partial}{\partial u^i}])\\ &= \overline{\mathrm{D}}_{\frac{\partial}{\partial u^i}}\widetilde{W}_t,\end{aligned} \tag{10}$$

where the Lie-bracket of $\frac{\partial}{\partial t}$ and $\frac{\partial}{\partial u^i}$ is $[\frac{\partial}{\partial t}, \frac{\partial}{\partial u^i}] = 0$ and $(\widetilde{\Phi}_t)_*([\frac{\partial}{\partial t}, \frac{\partial}{\partial u^i}]) = (\widetilde{\Phi}_t)_*(0) = 0$.

Hence, we gain the equation as follow:

$$\widetilde{V}'(t) = \int_{\widetilde{\mathcal{M}}_t} \sum_{i,j} (\widetilde{g}_t)^{ij} \langle \overline{\mathrm{D}}_{\frac{\partial}{\partial u^i}} \widetilde{W}_t, (X_t)_j \rangle \mathrm{d}\widetilde{\Omega}_t. \tag{11}$$

According to the formula

$$\langle \overline{\mathrm{D}}_{\frac{\partial}{\partial u^i}} \widetilde{W}_t, (X_t)_j \rangle = \frac{\partial}{\partial u^i} \langle \widetilde{W}_t, (X_t)_j \rangle - \langle \widetilde{W}_t, \overline{\mathrm{D}}_{\frac{\partial}{\partial u^i}} (X_t)_j \rangle, \tag{12}$$

we make a step further and get

$$\widetilde{V}'(t) = \int_{\widetilde{\mathcal{M}}_t} \sum_{i,j} (\widetilde{g}_t)^{ij} \Big[\frac{\partial}{\partial u^i} \langle \widetilde{W}_t, (X_t)_j \rangle - \langle \widetilde{W}_t, \overline{\mathrm{D}}_{\frac{\partial}{\partial u^i}} (X_t)_j \rangle \Big] \mathrm{d}\widetilde{\Omega}_t. \tag{13}$$

The Gauss formula (equation (5)) implies

$$\langle \widetilde{W}_t, \overline{\mathrm{D}}_{\frac{\partial}{\partial u^i}} (X_t)_j \rangle = \langle \widetilde{W}_t, (\widetilde{\Phi}_t)_* (\widetilde{\mathrm{D}}^t_{\frac{\partial}{\partial u^i}} \frac{\partial}{\partial u^i}) \rangle + \langle \widetilde{W}_t, h_t(\frac{\partial}{\partial u^i}, \frac{\partial}{\partial u^j}) \rangle, \tag{14}$$

then, we obtain

$$\widetilde{V}'(t) = \int_{\widetilde{\mathcal{M}}_t} \sum_{i,j} (\widetilde{g}_t)^{ij} \Big\{ \frac{\partial}{\partial u^i} \langle \widetilde{W}_t, (X_t)_j \rangle - \langle \widetilde{W}_t, (\widetilde{\Phi}_t)_* (\mathrm{D}^t_{\frac{\partial}{\partial u^i}} \frac{\partial}{\partial u^i}) \rangle - \langle \widetilde{W}_t, h_t(\frac{\partial}{\partial u^i}, \frac{\partial}{\partial u^j}) \rangle \Big\} \mathrm{d}\widetilde{\Omega}_t. \tag{15}$$

where h_t is the Second Fundamental Form of the submanifold $\widetilde{\mathcal{M}}_t$.

Lemma 1: $\sum_{i,j} (\widetilde{g}_t)^{ij} \Big\{ \frac{\partial}{\partial u^i} \langle \widetilde{W}_t, (X_t)_j \rangle - \langle \widetilde{W}_t, (\widetilde{\Phi}_t)_* (\widetilde{\mathrm{D}}^t_{\frac{\partial}{\partial u^i}} \frac{\partial}{\partial u^i}) \rangle \Big\}$ is the divergence of some tangent vector field $Y_t \in \mathcal{T}\mathcal{M}_t$.

Proof: Let

$$Y_t = \sum_{i,j} (\widetilde{g}_t)^{ij} \langle \widetilde{W}_t, (\widetilde{\Phi}_t)_* (\frac{\partial}{\partial u^j}) \rangle \frac{\partial}{\partial u^i}. \tag{16}$$

be a tangent vector field in $\mathcal{T}\mathcal{M}_t$. Then, after calculating the divergence of Y_t we have

$$\begin{aligned} \mathrm{div}(Y_t) &= \sum_{i,j} \frac{\partial ((\widetilde{g}_t)^{ij} (Y_t)_j)}{\partial u^i} + \sum_{i,j,k} (\widetilde{\Gamma}_t)^i_{ji} (g_t)^{jk} (Y_t)_k \\ &= \sum_{i,j} (\frac{\partial (\widetilde{g}_t)^{ij}}{\partial u^i} (Y_t)_j + (\widetilde{g}_t)^{ij} \frac{\partial (Y_t)_j}{\partial u^i}) + \sum_{i,j,k} (\widetilde{\Gamma}_t)^i_{ji} (\widetilde{g}_t)^{jk} (Y_t)_k \\ &= \sum_{i,j} (\widetilde{g}_t)^{ij} \Big\{ \frac{\partial (Y_t)_j}{\partial u^i} - \sum_k (\widetilde{\Gamma}_t)^k_{ij} (Y_t)_k \Big\} \\ &= \sum_{i,j} (\widetilde{g}_t)^{ij} \Big\{ \frac{\partial}{\partial u^i} \langle \widetilde{W}_t, (X_t)_j \rangle - \langle \widetilde{W}_t, (\widetilde{\Phi}_t)_* (\widetilde{\mathrm{D}}^t_{\frac{\partial}{\partial u^i}} \frac{\partial}{\partial u^i}) \rangle \Big\}. \end{aligned} \tag{17}$$

Thus, the proof is finished.

The mean curvature vector of the $\widetilde{\mathcal{M}}_t$ in ambient space is defined as follow:

$$\mathcal{H}_t = \sum_{i,j} \frac{1}{n} (\widetilde{g}_t)^{ij} h_t (\frac{\partial}{\partial u^i}, \frac{\partial}{\partial u^j}),$$

Taking $\mathcal{H}_t$ and $\mathrm{div}(Y_t)$ into equation (15), we obtain

$$\widetilde{V}'(t) = \int_{\widetilde{\mathcal{M}}_t} (\mathrm{div}(Y_t) - n \langle \mathcal{H}_t, \widetilde{W}_t \rangle) \mathrm{d}\widetilde{\Omega}_t, \tag{18}$$

Using the Divergence Theorem in [21] for manifolds, we have

$$\int_{\widetilde{\mathcal{M}}_t} \mathrm{div}(Y_t) \mathrm{d}\widetilde{\Omega}_t = - \int_{\partial \widetilde{\mathcal{M}}_t} \langle Y_t, n_t \rangle \mathrm{d}\widetilde{V}^t_{\partial \widetilde{\mathcal{M}}_t}, \tag{19}$$

since $\partial \widetilde{\mathcal{M}}_t = \varnothing$, $\int_{\widetilde{\mathcal{M}}_t} \mathrm{div}(Y_t) \mathrm{d}\widetilde{\Omega}_t = 0$, finally we obtain

$$\widetilde{V}'(t) = -n \int_{\widetilde{\mathcal{M}}_t} \langle \mathcal{H}_t, \widetilde{W}_t \rangle \mathrm{d}\widetilde{\Omega}_t. \tag{20}$$

Substituting $\widetilde{W}_t$ with $\alpha \mathcal{H}_t, \alpha > 0$, we have $\widetilde{V}'(t) = -n\alpha \int_{\widetilde{\mathcal{M}}_t} \langle \mathcal{H}_t, \mathcal{H}_t \rangle \mathrm{d}\widetilde{\Omega}_t$, for $\langle \mathcal{H}_t, \mathcal{H}_t \rangle > 0, \forall p \in \widetilde{\mathcal{M}}_t$, hence we get $\widetilde{V}'(t) < 0$. Thus, the proof is finished.

As we've proved, if the virtual manifold $\widetilde{\mathcal{M}}_t$ evolves exactly along the direction of $\mathcal{H}_t$, then the first order derivative of the volume $\widetilde{V}'(t) < 0$. As the consequence, the volume $\widetilde{V}(t)$ of the virtual manifold will decay. This finishes the proof, and we figure out the desired velocity field $\widetilde{W}_t$ for the virtual manifold. We will establish a second-order model for agents using these results in subsection III-B.

B. THE SECOND-ORDER MULTI-AGENT SYSTEM MODEL BASED ON MEAN CURVATURE VECTOR

In order to obtain the smooth flow map Ψ for the agents. The mean curvature vector $\mathcal{H}_t$ must be projected into the tangent space $T\mathcal{M}$ due to the evolution of agents is limited on the manifold $\mathcal{M}$. Moreover, agents are supposed to move in a shorter path, especially in geodesics when the projection of the mean curvature vector is zero. This means that if $\mathcal{P}(\mathcal{H}_t) = 0$, then the acceleration $\mathrm{D}_v v$ of the agents must be 0. Finally, a second-order dynamic model for the multi-agent system is obtained as follows:

$$\begin{cases} \mathrm{D}_v v &= \alpha \mathcal{P}(\mathcal{H}_t) \\ v &= \dfrac{\partial u}{\partial t} \\ v\big|_{t=0} &= v(0) \\ u\big|_{t=0} &= u(0) \end{cases} \quad \forall p \in \mathcal{M}, \tag{21}$$

where v, u are the velocity and position of the agent respectively, $\mathrm{D}_v v$ is the covariant derivative of v on $\mathcal{M}$, $\mathcal{H}_t$ is the mean curvature vector of the virtual manifold $\widetilde{\mathcal{M}}_t$, $\mathcal{P}$ is the projection operator that projects the vector into the tangent space of $\mathcal{M}_t$.

After some preliminary analysis, we can find that the solutions of system (21) will converge to a stable state asymptotically. This is because when the agents are very close to each other, the volume of a virtual manifold is very small, and $\|\mathcal{P}(\mathcal{H}_t)\|$ is close to 0; thus each agent moves in geodesic. These lead agents move far away from each other, then the norm of $\|\mathcal{P}(\mathcal{H}_t)\|$ increases, and agents aggregate together again under the effects of it. As a result, the accelerations and velocities descend to a small constant asymptotically. In order to verify our theoretical analysis, some simulations on sphere are performed in section IV.

IV. AGGREGATION OF MULTI-AGENT SYSTEM ON SPHERE

For definiteness, we consider the multi-agent's aggregation problem on sphere, which is commonly considered in applications. At first, we construct a virtual manifold according to our theory. Then, numerical simulations for a system of 100 agents on S^2 (sphere of 2-dimension) are performed, and some dynamic variables are analyzed.

A. CONSTRUCTION OF THE VIRTUAL MANIFOLD FOR S^2

The spherical coordination(ψ, θ), $\psi \in [0, \pi], \theta \in [0, 2\pi)$ is chosen to describe the position of agents on sphere. The smooth flow map of the original manifold S^2 is defined to be

$$\Phi_t : (\psi, \theta) \to (\sin\psi\cos\theta, \sin\psi\sin\theta, \cos\psi). \tag{22}$$

The tangent space $\mathcal{T}S^2$ is consisted with two vectors as follow:

$$\frac{\partial}{\partial\psi} = (\cos\psi\cos\theta, \cos\psi\sin\theta, -\sin\psi)$$
$$\frac{\partial}{\partial\theta} = (-\sin\psi\sin\theta, \sin\psi\cos\theta, 0).$$

In $\mathbb{R}^3$, we have the equation $\mathcal{H}_t = \lambda_t N_t$, where N_t is the normal vector of $\mathcal{M}$. In order to make the agents aggregate to the centroid of the system, we construct a virtual manifold $\widetilde{\mathcal{M}}_t$ with geometric intuition as follow:

$$\widetilde{\Phi}_t : (\psi, \theta) \to (\widetilde{\phi}_t \sin\psi\cos\theta, \widetilde{\phi}_t \sin\psi\sin\theta, \widetilde{\phi}_t \cos\psi) \tag{23}$$

where

$$\widetilde{\phi}_t(\theta, \psi) = \beta[1 + \sin(\frac{3\pi}{2} + \frac{d_{p,p_c}}{2})], 0 \leq d_{p,p_c} \leq \pi. \tag{24}$$

$d_{p,p_c} = \arccos(\cos\psi\cos\psi_c + \cos(\theta - \theta_c)\sin\psi\sin\psi_c)$ is the geodesic distance between $p = (\psi, \theta)$ and the centroid point of the system is $p_c = (\psi_c, \theta_c)$. $\theta_c = \frac{\sum_i \theta_i}{N}$ and $\psi_c = \frac{\sum_i \psi_i}{N}$.

Then, the Riemannian metric $\widetilde{g}_t$ of $\widetilde{\mathcal{M}}_t$ is carried out to be

$$\begin{aligned} (\widetilde{g}_t)_{\theta\theta} &= (\widetilde{\phi}_t)^2 \sin^2\psi + (\frac{\partial\widetilde{\phi}_t}{\partial\theta})^2 \\ (\widetilde{g}_t)_{\theta\psi} &= \frac{\partial\widetilde{\phi}_t}{\partial\theta}\frac{\partial\widetilde{\phi}_t}{\partial\psi} \\ (\widetilde{g}_t)_{\psi\psi} &= (\frac{\partial\widetilde{\phi}_t}{\partial\psi})^2 + \widetilde{\phi}_t^2. \end{aligned} \tag{25}$$

The mean curvature vector $\mathcal{H}_t$ is calculated using the equation

$$\mathcal{H}_t = \Delta_{\widetilde{\mathcal{M}}_t}\widetilde{\Phi}_t = \begin{pmatrix} (\widetilde{g}_t)^{ij}\frac{\partial^2\widetilde{\Phi}_t^1}{\partial x^i\partial x^j} - \sum_{l=1}^n(\widetilde{g}_t)^{ij}(\widetilde{\Gamma}_t)_{ij}^l\frac{\partial\widetilde{\Phi}_t^1}{\partial x^l} \\ \vdots \\ (\widetilde{g}_t)^{ij}\frac{\partial^2\widetilde{\Phi}_t^k}{\partial x^i\partial x^j} - \sum_{l=1}^n(\widetilde{g}_t)^{ij}(\widetilde{\Gamma}_t)_{ij}^l\frac{\partial\widetilde{\Phi}_t^k}{\partial x^l} \\ \vdots \\ (\widetilde{g}_t)^{ij}\frac{\partial^2\widetilde{\Phi}_t^{n+1}}{\partial x^i\partial x^j} - \sum_{l=1}^n(\widetilde{g}_t)^{ij}(\widetilde{\Gamma}_t)_{ij}^l\frac{\partial\widetilde{\Phi}_t^{n+1}}{\partial x^l} \end{pmatrix}. \tag{26}$$

and the projection of mean curvature vector $\mathcal{P}(\mathcal{H}_t)$ to the tangent space TS^2 is figured out to be:

$$\mathcal{P}(\mathcal{H}_t) = \langle\mathcal{H}_t, \frac{\partial}{\partial\psi}\rangle\frac{\partial}{\partial\psi} + \langle\mathcal{H}_t, \frac{\partial}{\partial\theta}\rangle\frac{\partial}{\partial\theta}. \tag{27}$$

In order to verify our approach, some simulations are performed in next subsection.

B. NUMERICAL SIMULATION OF AGGREGATION BEHAVIOR ON S^2

The initial positions $\{p_i\}_{i=1}^N$ of agents are randomly chosen on S^2 with $\|p_i(t)\| = 1$, and the initial velocities $\{v_i\}_{i=1}^N$ are randomly generated from the tangent space TS^2 with norms ranging from 0.1 to 0.5. After many repeated experiments, some good combinations of parameters in our system were found. The parameter in the ordinary system (21) is set to be $\alpha = 10$, and the parameter in construction of virtual manifold in equation (24) is set to be $\beta = -2$. Since the system evolves on the sphere, with $\|p_i(t)\| = 1, \forall i = 1, \cdots, N, \forall t \in [0, \infty)]$, the norm of centroid $\|p_c(t)\| = \|\sum_i \frac{p_i(t)}{N}\|$ can be used to approximate the volume of the system. If the agents aggregate to an identical point, we have $\lim_{t\to+\infty}\|p_c(t)\| = 1$, otherwise, $\lim_{t\to+\infty}\|p_c(t)\| = 0$ as distance among agents grows. Therefore, this quantity is considered as the criterion of agents' aggregation in [10]. Besides, position variance and its logarithm also reflect the system's volume, and both are plotted in our simulation results. Moreover, in order to analyze the dynamic of agents, the evolution of velocities $\{\|v_i\|\}_{i=1}^N$ and logarithm of accelerations $\{a_i = \mathcal{P}(\mathcal{H}_t)\}_{i=1}^N$ are also plotted. In order to illustrate our approach, the virtual manifold at $t = 0s$ is plotted in Fig 1. As time goes by, the virtual manifold will change according to the movements of agents.

From Fig 2(a) to Fig 2(b), the positions of the agents at different times are plotted. The red plane represents the agent, the blue arrow indicates the mean curvature vector

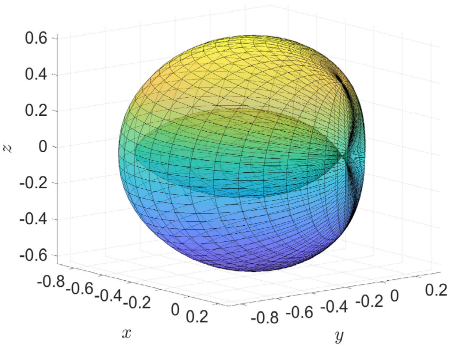

FIGURE 1. Time-varying virtual manifold $\widetilde{\mathcal{M}}_t$.

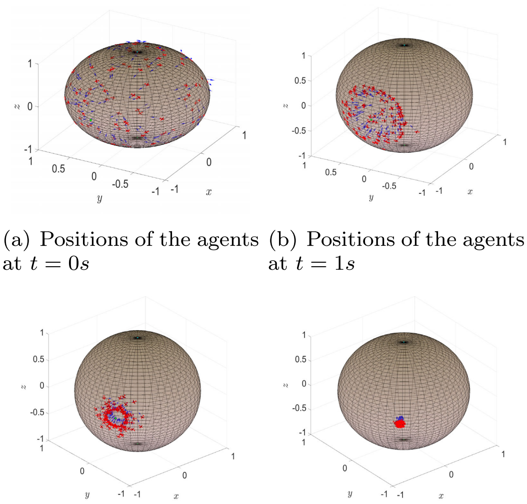

(a) Positions of the agents at $t = 0s$ (b) Positions of the agents at $t = 1s$

(c) Positions of the agents at $t = 5s$ (d) Positions of the agents at $t = 100s$

FIGURE 2. Evolution of Multi-agent system on S^2.

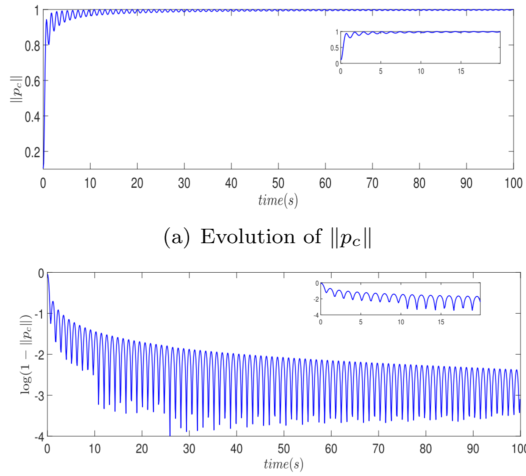

(a) Evolution of $\|p_c\|$

(b) Evolution of $\log(1 - \|p_c\|)$

FIGURE 3. Evolution of $\|p_c\|$ and $\log(1 - \|p_c\|)$ on sphere.

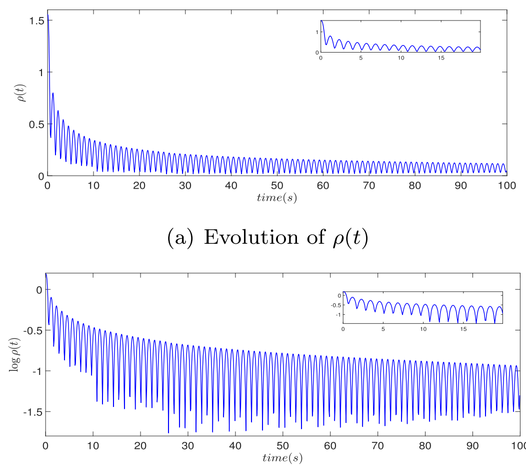

(a) Evolution of $\rho(t)$

(b) Evolution of $\log \rho(t)$

FIGURE 4. Evolution of $\rho(t)$ and $\log \rho(t)$ on sphere.

and the green dot designates the centroid of agents in these figures. We can find that agents aggregate to an identical point asymptotically. This confirms the analytical results in section III.

In Fig 3, we plot the norm of the centroid $p_c(t)$, and we can see, $\|p_c(t)\|$ approaches 1 asymptotically as time goes to infinity. It means that agents collect to an exact point asymptotically. In Fig 3(a), since $\|p_c(t)\|$ is very close to 1, we plot $\log(1 - \|p_c(t)\|)$ to show the increasing of $\|p_c(t)\|$ more clearly. The value of $\log(1 - \|p_c(t)\|)$ decays asymptotically, and it also implies that $\lim_{t\to+\infty} \|p_c(t)\| = 1$. Both the two variables show that the agents aggregate asymptotically as time goes by.

In Fig 4(a) and Fig 4(b), we plotted the position variance and the logarithm of the position variance of agents, respectively. Besides the norm of centroid point $\|p_c(t)\|$, position variance $\rho(t)$ also plays a significant role in describing the dynamics of the system. As we can see in the figures, the position variance decrease to zero asymptotically, and the logarithm of position variance goes down to $-\infty$ asymptotically, which exactly meets the analytical result. This result also implies agents aggregate together asymptotically.

In Fig 5(a) and Fig 5(b), we plot the norm of velocities $v_i(t) = (\dot{\psi}_i(t), \dot{\theta}_i(t))$ and the logarithm of norm of velocities $\log \|v_i(t)\|$ of agents respectively. From the figures above, we can see that the norm of velocities decreases to a small constant asymptotically with an unknown rate, and the norm of the velocities becomes identical asymptotically. This result implies that different agents' behavior tends to be consistent asymptotically.

Finally, in order to analyze the acceleration of agents at different stages, the evolution of $\|\mathcal{P}(\mathcal{H}_t)\|$ is plotted in Fig 5(c). From the picture above, we can see that the norm of accelerations decreases to a small value asymptotically, which is consistent with the evolution of the velocities of

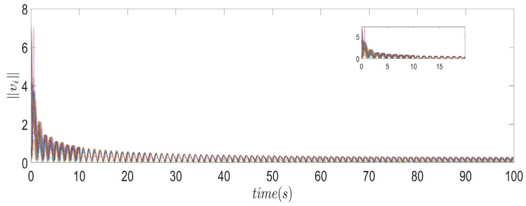

(a) Norm of velocities $\{\|v_i\|\}_{i=1}^N$

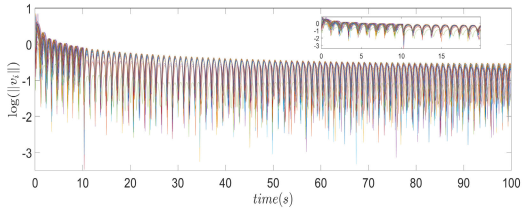

(b) Logarithm of norm of velocities $\{\log(\|v_i\|)\}_{i=1}^N$

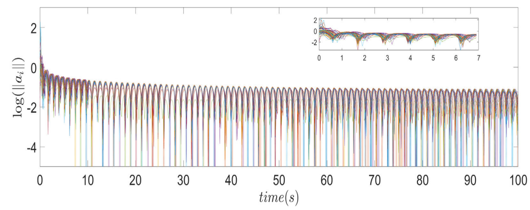

(c) Evolution of accelerations $\{\|a_i\|\}_{i=1}^N$

FIGURE 5. Evolution of the multi-agent system's velocities and accelerations on S^2.

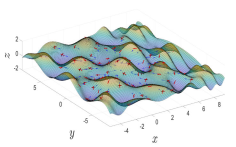

(a) Positions of the agents at $t = 0s$

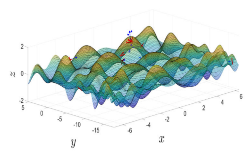

(b) Positions of the agents at $t = 5s$

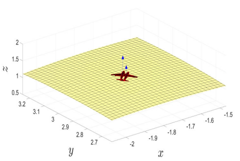

(c) Positions of the agents at $t = 50s$

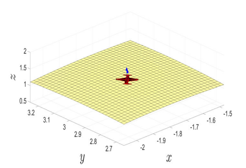

(d) Positions of the agents at $t = 200s$

FIGURE 6. Evolution of Multi-agent system on a non-homogeneous manifold.

agents. Once again, this consequence implies that different agents' behaviors tend to be synergistic asymptotically.

It is obvious to observe that oscillations occur in all of these quantities we plotted. This is because when the agents are very close to each other, $\|\mathcal{P}(\mathcal{H}_t)\|$ is close to 0; thus, each agent moves in geodesic, and agents move far away from each other, then, the norm of $\|\mathcal{P}(\mathcal{H}_t)\|$ increases and agents aggregate together under the effects of $\mathcal{P}(\mathcal{H}_t)$. As a result, all of these dynamic variables will converge to a constant asymptotically.

C. NUMERICAL SIMULATION OF AGGREGATION BEHAVIOR ON A NON-HOMOGENEOUS MANIFOLD

In order to the advantages of our approach over the second-order Kuramoto model in [10], we implement our approach for multi-agent system moving on a hilly terrain-like manifold, which is a non-homogeneous surface with many peaks. Cartesian coordinates (x, y) is chosen as the local charts, and the basis of the tangent space $\mathcal{TM}$ is $\{\frac{\partial}{\partial x}, \frac{\partial}{\partial y}\}$. The ambient space is embedded into $\mathbb{R}^3$ with the map defined as follow:

$$(x, y) \to (x, y, \sin x \cos y + 0.5 \sin 0.3x^2 \cos 0.1y^2). \quad (28)$$

The tangent vector is carried out to be

$$\frac{\partial}{\partial x} = (1, 0, \cos x \cos y + 0.3x \cos 0.3x^2 \cos 0.1y^2)$$
$$\frac{\partial}{\partial y} = (0, 1, -\sin x \sin y - 0.1y \sin 0.3x^2 \sin 0.1y^2)$$

With the results in section III, the virtual manifold $\widetilde{\mathcal{M}}_t$ is constructed through the smooth flow map $\widetilde{\Phi}_t$ as follow:

$$(x, y) \to (x, y, \beta[(x - x_c)^2 + (y - y_c)^2]^\gamma). \quad (29)$$

where (x_c, y_c), $x_c = \frac{\sum_i x_i}{N}$, $y_c = \frac{\sum_i y_i}{N}$ is the centroid point of the multi-agent system. The Riemann metric $\widetilde{g}_t$ of $\widetilde{\mathcal{M}}_t$ is

$$(\widetilde{g}_t)_{xx} = 1 + (2\beta\gamma(x - x_c)[(x - x_c)^2 + (y - y_c)^2]^{\gamma-1})^2$$
$$(\widetilde{g}_t)_{xy} = 4\beta^2\gamma^2(x - x_c)(y - y_c)[(x - x_c)^2 + (y - y_c)^2]^{2\gamma-2}$$
$$(\widetilde{g}_t)_{yy} = 1 + (2\beta\gamma(y - y_c)[(x - x_c)^2 + (y - y_c)^2]^{\gamma-1})^2. \quad (30)$$

The mean curvature vector $\mathcal{H}_t$ is calculated using the equation (26) and the projection of mean curvature vector $\mathcal{P}(\mathcal{H}_t)$ to the tangent space $T\mathcal{M}_t$ is figured out to be:

$$\mathcal{P}(\mathcal{H}_t) = \langle \mathcal{H}_t, \frac{\partial}{\partial x} \rangle \frac{\partial}{\partial x} + \langle \mathcal{H}_t, \frac{\partial}{\partial y} \rangle \frac{\partial}{\partial y}. \quad (31)$$

1) SYSTEM PARAMETERS AND THE SIMULATION RESULTS

The initial positions $\{x_i\}_{i=1}^N$ of agents is randomly chosen on $\mathcal{M}$, and each component of initial velocities $\{v_i\}_{i=1}^N$ are randomly generated from the tangent space $T\mathcal{M}$ with range from 0.5 to 2. In our simulations, the parameter in the ordinary system (21) is set to be $\alpha = 200$, and the parameters in equation (29) is set to be $\beta = 5, \gamma = 1.5$.

In Fig 6, we plot the positions of agents at different times $t = 0s$, $t = 5s$, $t = 50s$, $t = 200s$ (the red planes represent the positions of the agents and the blue arrows designate the mean curvature vectors). We can see that the agents is randomly distributed in the manifold at $t = 0s$, and the agents aggregate to an identical point as time goes to infinity. This result implies the system aggregate asymptotically as time goes by.

Since the norm of centroid point is not suitable to describe the aggregation dynamic of agents evolves on the non-compact manifold $\mathcal{M}$, we need other quantities to describe

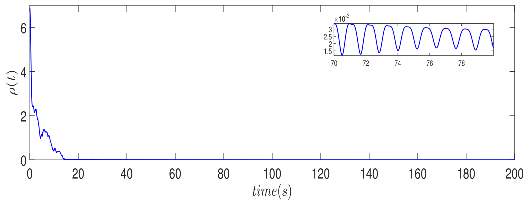

(a) Evolution of $\rho(t)$

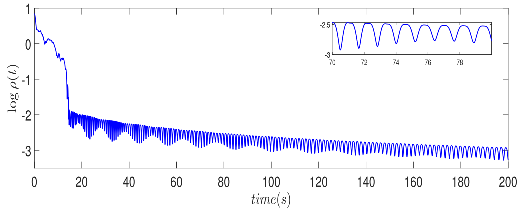

(b) Evolution of $\log \rho(t)$

FIGURE 7. Evolution of $\rho(t)$ and $\log \rho(t)$ on a non-homogeneous manifold.

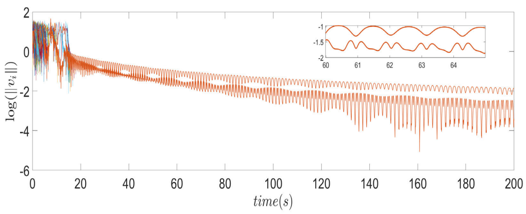

(a) Logarithm of norm of velocities $\{\log(\|v_i\|)\}_{i=1}^{N}$

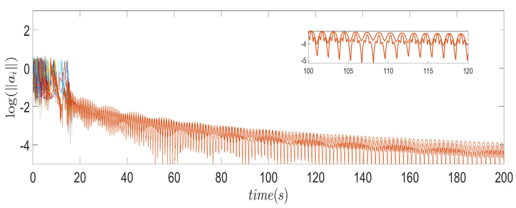

(b) Evolution of accelerations $\{\|a_i\|\}_{i=1}^{N}$

FIGURE 8. Evolution of the multi-agent system's velocities and accelerations on a non-homogeneous manifold.

the aggregation dynamic of the system. In Fig 7(a) and Fig 7(b), we plot the position variance and the logarithm of position variance respectively. As the Fig 7(b) represents, the position variance $\rho(t) = \sum_{i,j=1}^{N} \frac{\sqrt{(x_i - x_j)^2}}{N^2}$ descends at first and tends to zero asymptotically, which is consistent with our analytical conclusion $\lim_{t\to\infty} V(t) = 0$, thus implying the agents evolve to aggregate asymptotically. The logarithm of position variance descends to zero asymptotically. Both of the results confirm that the multi-agent system reach a aggregation state.

In Fig 8(a), we plot the logarithm of velocities' norm $\{\|v_i\|\}_{i=1}^{N}$ of the agents. From the figures above, we can see that the norms of velocities decrease to a small constant asymptotically with an unknown rate, and the norm of the velocities become identical gradually; this implies all of the agents in the system evolve in the same way, thus, leading to aggregation behaviors. The evolution of accelerations' norm of agents is represented by log plot in Fig 8(b). We can find that the velocities and accelerations of the agents have the same dynamic behaviors, and both two variables converge to a small constant asymptotically. The numerical results are consistent with our theory analysis in III and, especially, the results on the sphere are consistent with that of the second-order Kuramoto model on the sphere.

V. CONCLUSION

In this paper, firstly, we use the local charts to describe the manipulation of the agents on manifolds. The local charts make the agents satisfy geometric constraints naturally. Then, we convert the aggregation problem of agents on manifolds into an optimization issue of minimizing the virtual manifold's volume. We show that the mean curvature field will minimize the volume of the virtual manifolds. Furthermore, we propose a novel approach describing the multi-agent system's aggregation behaviors on general manifolds with the mean curvature fields. To this end, we implement our approach to the multi-agent system's aggregation on the sphere and a non-homogeneous manifold. Finally, we perform some numerical simulations, and the corresponding numerical results are consistent with our theoretical analysis. The numerical results show that our approach has the same results in [10] on the sphere and has excellent performance on a non-compact and non-homogeneous manifold. In conclusion, our approach properly describes agents' aggregation behaviors on general manifolds without adding additional equations or other terms which is used to make the motion of agent confined to the ambient spaces to our model. What' more, the implementation of our approach on describing other synergistic behaviors of multi-agent systems on manifolds will also be considered in our future works and there still many interesting but difficult issues that are still unsolved; such as the collective behaviors of multi-agents moving on manifolds with switchable topology, time delays and various communication methods.

REFERENCES

[1] R. Olfati-Saber, "Flocking for multi-agent dynamic systems: Algorithms and theory," *IEEE Trans. Autom. Control*, vol. 51, no. 3, pp. 401–420, Mar. 2006, doi: 10.1109/TAC.2005.864190.

[2] O. Khatib, "Real-time obstacle avoidance for manipulators and mobile robots," in *Proc. IEEE Int. Conf. Robot. Autom.*, Mar. 1985, pp. 500–505, doi: 10.1109/ROBOT.1985.1087247.

[3] A. Czirok, A. Barabasi, and T. Vicsek, "Collective motion of self-propelled particles: Kinetic phase transition in one dimension," *Phys. Rev. Lett.*, vol. 82, no. 1, pp. 209–212, 1999, doi: 10.1103/PhysRevLett.82.209.

[4] T. Vicsek, A. Czirók, E. Ben-Jacob, I. Cohen, and O. Shochet, "Novel type of phase transition in a system of self-driven particles," *Phys. Rev. Lett.*, vol. 75, no. 6, pp. 1226–1229, Aug. 1995, doi: 10.1103/PhysRevLett.75.1226.

[5] W. Li, "Collective motion of swarming agents evolving on a sphere manifold: A fundamental framework and characterization," *Sci. Rep.*, vol. 5, no. 1, Sep. 2015, Art. no. 13603, doi: 10.1038/srep13603.

[6] D. Chi, S.-H. Choi, and S.-Y. Ha, "Emergent behaviors of a holonomic particle system on a sphere," *J. Math. Phys.*, vol. 55, no. 5, May 2014, Art. no. 052703, doi: 10.1063/1.4878117.

[7] M. A. Lohe, "Non-Abelian Kuramoto models and synchronization," *J. Phys. A, Math. Theor.*, vol. 42, no. 39, pp. 395101–395126, Sep. 2009.

[8] S.-Y. Ha, M. Kang, and D. Kim, "Emergent behaviors of high-dimensional Kuramoto models on Stiefel manifolds," *Automatica*, vol. 136, Feb. 2022, Art. no. 110072, doi: 10.1016/j.automatica.2021.110072.
[9] F. Cucker and S. Smale, "Emergent behavior in flocks," *IEEE Trans. Autom. Control*, vol. 52, no. 5, pp. 852–862, May 2007, doi: 10.1109/TAC.2007.895842.
[10] S.-Y. Ha and D. Kim, "A second-order particle swarm model on a sphere and emergent dynamics," *SIAM J. Appl. Dyn. Syst.*, vol. 18, no. 1, pp. 80–116, Jan. 2019, doi: 10.1137/18M1205996.
[11] S.-Y. Ha, D. Kim, and F. W. Schloder, "Emergent behaviors of Cucker–Smale flocks on Riemannian manifolds," *IEEE Trans. Autom. Control*, vol. 66, no. 7, pp. 3020–3035, Jul. 2021, doi: 10.1109/TAC.2020.3014096.
[12] S.-Y. Ha, D. Ko, and S. W. Ryoo, "On the relaxation dynamics of Lohe oscillators on some Riemannian manifolds," *J. Stat. Phys.*, vol. 172, no. 5, pp. 1427–1478, Sep. 2018, doi: 10.1007/s10955-018-2091-0.
[13] H. Ahn, S.-Y. Ha, M. Kang, and W. Shim, "Emergent behaviors of relativistic flocks on Riemannian manifolds," *Phys. D, Nonlinear Phenomena*, vol. 427, Dec. 2021, Art. no. 133011, doi: 10.1016/j.physd.2021.133011.
[14] J. R. Goodman and L. J. Colombo, "Collision avoidance of multiagent systems on Riemannian manifolds," *SIAM J. Control Optim.*, vol. 60, no. 1, pp. 168–188, Feb. 2022, doi: 10.1137/21M1411056.
[15] J. Markdahl, "Synchronization on Riemannian manifolds: Multiply connected implies multistable," *IEEE Trans. Autom. Control*, vol. 66, no. 9, pp. 4311–4318, Sep. 2021, doi: 10.1109/TAC.2020.3030849.
[16] A. Bloch, M. Camarinha, and L. J. Colombo, "Dynamic interpolation for obstacle avoidance on Riemannian manifolds," *Int. J. Control*, vol. 94, no. 3, pp. 588–600, Mar. 2021, doi: 10.1080/00207179.2019.1603400.
[17] A. Aydoğdu, S. T. McQuade, and N. P. Duteil, "Opinion dynamics on a general compact Riemannian manifold," *Netw. Heterogeneous Media*, vol. 12, no. 3, pp. 489–523, 2017, doi: 10.3934/nhm.2017021.
[18] T. Beckers and L. J. Colombo and S. Hirche, "On the relaxation dynamics of Lohe oscillators on some Riemannian manifolds," *J. Geometric Mech.*, vol. 14, no. 4, pp. 491–505, 2022, doi: 10.3934/jgm.2022018.
[19] R. C. Fetecau and B. Zhang, "Self-organization on Riemannian manifolds," *J. Geometric Mech.*, vol. 11, no. 3, pp. 397–426, 2019, doi: 10.3934/jgm.2019020.
[20] J. M. Lee, *Riemannian Manifolds: An Introduction to Curvature*, vol. 176, 1st ed. New York, NY, USA: Springer, 1997, pp. 23–153, doi: 10.1007/b98852.
[21] S. Gallot, D. Hulin, and J. Lafontaine, *Riemannian Geometry*, 3rd ed. Berlin, Germany: Springer, 2004, pp. 51–262, doi: 10.1007/978-3-642-18855-8.
[22] J. M. Lee, *Introduction to Smooth Manifolds*, vol. 218, 2nd ed. New York, NY, USA: Springer, 2012, pp. 1–439, doi: 10.1007/978-1-4419-9982-5.

LUNXIAO TANG received the B.S. degree in applied mathematics from the College of Mathematics, Sichuan University, Chengdu, China, in 2019, where he is currently pursuing the Ph.D. degree with the College of Mathematics. His research interests include Riemannian geometry, swarm intelligence, and control of multi-agent systems.

TAO YU received the B.S., M.S., and Ph.D. degrees from the College of Mathematics, Sichuan University, Chengdu, China, in 2008, 2010, and 2013, respectively. She is currently an Associate Professor with the College of Mathematics, Sichuan University. Her research interests include dynamical system theory, swarm intelligence, and optimization problems on optical networks.

MAOKANG LUO received the B.S. degree from the School of Mathematical Sciences, University of Science and Technology of China, Hefei, China, in 1981, and the M.S. and Ph.D. degrees from the College of Mathematics, Sichuan University, Chengdu, China, in 1984 and 1992, respectively. He is currently a Professor with the College of Mathematics, Sichuan University. His research interests include artificial intelligence, topology and geometry, and fuzzy mathematics.